AFRL-RV-PS-
TR-2012-0035

GENERATION OF HIGH-FREQUENCY P AND S WAVE RADIATION FROM UNDERGROUND EXPLOSIONS

Charles G. Sammis

University of Southern California
Department of Earth Sciences
Los Angeles, CA 90089-0740

30 December 2011

Final Report

AIR FORCE RESEARCH LABORATORY
Space Vehicles Directorate
3550 Aberdeen Ave SE
AIR FORCE MATERIEL COMMAND
KIRTLAND AIR FORCE BASE, NM 87117-5776

DTIC COPY

NOTICE AND SIGNATURE PAGE

Using Government drawings, specifications, or other data included in this document for any purpose other than Government procurement does not in any way obligate the U.S. Government. The fact that the Government formulated or supplied the drawings, specifications, or other data does not license the holder or any other person or corporation; or convey any rights or permission to manufacture, use, or sell any patented invention that may relate to them.

This report was cleared for public release by the Air Force Research Laboratory 377 ABW Public Affairs Office and is available to the general public, including foreign nationals. Copies may be obtained from the Defense Technical Information Center (DTIC) (http://www.dtic.mil).

AFRL-RV-PS-TR-2012-0035 HAS BEEN REVIEWED AND IS APPROVED FOR PUBLICATION IN ACCORDANCE WITH ASSIGNED DISTRIBUTION STATEMENT.

//signed//	//signed//
Robert Raistrick, RVBYE Project Manager	Joel B. Mozer Chief, AFRL/RVB

This report is published in the interest of scientific and technical information exchange, and its publication does not constitute the Government's approval or disapproval of its ideas or findings.

REPORT DOCUMENTATION PAGE

Form Approved
OMB No. 0704-0188

1. REPORT DATE *(DD-MM-YYYY)*	2. REPORT TYPE	3. DATES COVERED *(From - To)*
30-12-2011	Final Report	16 Apr 2008 to 15 Oct 2011

4. TITLE AND SUBTITLE
Generation of High-Frequency P and S Wave Radiation from Underground Explosions

5a. CONTRACT NUMBER
FA8718-08-C-0026

5b. GRANT NUMBER

5c. PROGRAM ELEMENT NUMBER
62601F

6. AUTHOR(S)
Charles G. Sammis

5d. PROJECT NUMBER
1010

5e. TASK NUMBER

5f. WORK UNIT NUMBER
837136

7. PERFORMING ORGANIZATION NAME(S) AND ADDRESS(ES)

University of Southern California
Department of Earth Sciences
Los Angeles, CA 90089-0740

8. PERFORMING ORGANIZATION REPORT NUMBER

9. SPONSORING / MONITORING AGENCY NAME(S) AND ADDRESS(ES)

Air Force Research Laboratory
Space Vehicles Directorate
3550 Aberdeen Ave SE
Kirtland AFB, NM 87117-5776

10. SPONSOR/MONITOR'S ACRONYM(S)
AFRL/RVBYE

11. SPONSOR/MONITOR'S REPORT NUMBER(S)
AFRL-RV-PS-TR-2012-0035

12. DISTRIBUTION / AVAILABILITY STATEMENT

Approved for public release; distribution is unlimited. (377ABW-2012-0113 dtd 01 Feb 2012)

13. SUPPLEMENTARY NOTES

14. ABSTRACT

The quasistatic damage mechanics formulated by Ashby and Sammis has been made fully dynamic by incorporating the results of recent experimental and theoretical studies of dynamic crack growth. The model has been verified by building it into the ABAQUS dynamic finite element code and using it to simulate high-speed fracture experiments. Simulation of explosions has shown that the spatial extent and pattern of the resultant fracture damage is sensitive to loading rate. High loading rates of short duration produce spherically symmetric compact damage patterns. Slower loading rates of longer duration are more effective in producing long radial fractures. Any asymmetry in the pattern of such radial fractures generates S wave radiation in the far-field, even in the absence of other factors known to generate S waves such as tectonic shear stress or anisotropy in the initial fracture distribution.

15. SUBJECT TERMS
Shear waves, Seismic sources, Model seismology, P and S wave radiation

16. SECURITY CLASSIFICATION OF: Fill in according to classification of report.			17. LIMITATION OF ABSTRACT	18. NUMBER OF PAGES	19a. NAME OF RESPONSIBLE PERSON
a. REPORT	b. ABSTRACT	c. THIS PAGE			Robert Raistrick
UNCLASSIFIED	UNCLASSIFIED	UNCLASSIFIED	Unlimited	22	19b. TELEPHONE NUMBER *(include area code)*

Standard Form 298 (Rev. 8-98)
Prescribed by ANSI Std. Z39.18

This page intentionally left blank.

Table of Contents

1. INTRODUCTION 1
2. BACKGROUND 2
3. METHODS, ASSUMPTIONS, AND PROCEDURES 4
3.1. Extending Micromechanical Damage Mechanics to High Loading Rates 7
3.2. Experimental Validation of Dynamic Damage Mechanics 9
4. RESULTS AND DISCUSSION 10
5. CONCLUSIONS 14
REFERENCES 15

List of Figures

1. Geometry in the Micromechanical Damage Mechanics Model 6

2. Temporal Evolution of the Dynamic Stress Intensity Factor.....8

3. Normalized Dynamic Stress Intensity Factors for Several Materials 9

4. Comparison Between Experimental Measurements and Model Predictions 9

5. Dynamic Damage Created by Different Loading Regimes 11

6. Damage Mapped in the Source of a Nuclear Explosion 12

7. Damage in a Glass Plate Produced by a Hypervelocity Impact.....12

8. Displacement Fields Generated by Fast Loading (left) and Slow Loading (right) 13

1. INTRODUCTION

The most successful discriminants between small underground explosions and low magnitude earthquakes are usually based on the ratio Pn/Lg or Pg/Lg since these wave trains tend to dominate short-period records observed in continental areas. Pn are compression waves critically refracted at the moho. The Lg train is S wave energy trapped in the "granitic" upper crust. It can be modeled as multiple total internal reflection of SH [1], or as a sum of higher-mode surface waves [2]. Similarly, the Pg wave train is trapped P wave energy. The ratios Pn/Lg and Pg/Lg begin to discriminate between explosions and earthquakes at frequencies above 1Hz and appear to work better with increasing frequency up to about 9 Hz [3].

There is a simple rational for using a P/S ratio to discriminate between explosions and earthquakes. An underground explosion is, to a first approximation, a spherically symmetric pressure source that is expected to generate mostly P waves. An earthquake is a shear slip along a fault plane that should generate mostly S waves. The ratio Pn/Lg should be larger for explosions than for earthquakes. While this is generally true, there are numerous exceptions that must be understood if this discriminant is to be widely used in different geological and tectonic environments. The two obvious sources of uncertainty in Pn/Lg are source effects and path effects. Our work has focused on understanding the source effects. In specific, we have investigated mechanisms by which explosions generate high-frequency P and S waves and how they depend on rock type in the source region, overburden, and tectonic regime. As discussed in more detail below, our approach has been to develop a micromechanical model for the dynamic generation of distributed fracturing (damage) in the non-linear source region of underground explosions, and to use this model in numerical simulations of explosions to quantitatively assess the role of fracture damage in the generation of P and S waves in the far field.

Our micromechanical damage mechanics model differs from the more commonly used continuum models in that we model the nucleation growth and interaction of the myriad of fractures driven by the high stresses in the source region. As we show in more detail below, this allows us to physically incorporate variables such as the initial fracture distribution in the source rock and loading-rate effects that are known strongly affect S wave generation.

2. BACKGROUND

The observed generation of S waves by a spherical explosion source was first explained as resulting from the dynamical relaxation of the cavity in a shear pre-stress field [4] [5] [6]. Shear wave radiation thus generated should have a dominant wavelength near the size of the explosion-generated cavity. More recently, Johnson and Sammis [7] have shown that the nucleation and growth of fractures in the source regime can also produce significant coherent P and S waves in the far-field. Pre-existing tectonic shear stress and/or a preferential orientation of the preexisting fractures that nucleate the explosion-induced fractures enhances the S energy. The difference between this new "fracture-damage" mechanism and the older relaxation mechanism is that the scale of the fracture sources can be much smaller so the resultant P and S energy can be high-frequency. We called this fracture-generated energy "secondary radiation" since it is not included in current seismic source models.

As detailed in the following section, we have recently improved the Ashby and Sammis model [8] by including high-velocity crack nucleation and growth laws, and have improved the Johnson and Sammis [7] analysis by building our new dynamic damage mechanics into the commercial ABAQUS dynamic finite element code. These improvements allow us to properly calculate the nucleation and growth of fracture damage at the extremely high loading rates in the non-linear source region of a nuclear explosion. Also, use of the ABAQUS code allows us represent the change in elastic stiffness associated with the damage in a physical way that is consistent with the damage mechanics, rather than using the ad hoc "effective elasticity" approach taken by Johnson and Sammis [7].

There is mounting observational evidence that P/S discriminants are strongly influenced by conditions at the source. Walters et al. [3] compared the signals from 130 underground nuclear explosions, one very large chemical explosion, and 50 earthquakes ranging in magnitude from 2 to 6. Since the instruments and propagation paths were roughly the same for these events, they were able to focus on source effects. For the explosions they investigated the effects of magnitude, depth, and working point properties of density, velocity, and gas porosity. The gas porosity also gives some information about effects associated with the water table since water saturated rock has zero gas porosity. Their conclusion was that Pn/Lg and Pg/Lg were more

sensitive to properties of the source medium than to the depth. Since velocity and density are strongly correlated with the gas porosity, it was not possible to determine which had the largest effect. The ratio tended to be larger in harder rock having lower gas porosity, with Pg/Lg showing a larger dependence than Pn/Lg. Walters et al. [3] also explored the relative excitation of Pn, Pg, and Lg at 1Hz with excitation of the same phase at 6-8 Hz for both explosions and earthquakes. For all phases, explosions in media with high gas porosity generated relatively less high frequency energy. They did not offer any physical explanation for these observations.

Xie and Patton [9] used a more formal inversion algorithm to separate source effects from propagation for the Pn and Lg phases from Lop Nor explosions and nearby earthquakes. They concluded that "spectral overshoot for explosions, differences in corner frequencies for Pn and Lg waves, and scaling relation for key spectral parameters are significant factors controlling the performance of the P/Lg discriminants for small to moderate events in central Asia." They also comment, "It is important to point out that in this paper we made no attempt to identify physical processes such as cavity rebound, spall, near source scattering, and interactions between pP and P, … that may be responsible for important spectral features of regional phases". To this list of physical processes we propose to add secondary radiation generated during rock fracture in the source and to investigate its contribution using our model.

Stevens et al. [10] considered four candidate mechanisms for explosion generated Lg:

1) "Direct generation by the explosion source where the explosion is modeled as a point compressional source."
2) "Secondary generation by the explosion source, where Lg is generated primarily by the nonspherical parts of the explosion source, with strong influence from the free surface."
3) "Rg scattering. The hypothesis is that the Rg phase is scattered as it travels away from the explosion and is converted to Lg."
4) "P scattering. The hypothesis is that Rg is in a sense a variant on P coda containing converted P->S phases in the crust."

They favored explanation 2. Explanation 1 was eliminated because the spherical source generates very little Lg. Explanation 3 was eliminated because Rg was observed to persist to large distances. They found that inclusion of a CLVD source with about half the strength of the

explosion generates the observed Lg. This is approximately the strength of the secondary radiation calculated by Johnson and Sammis [7] for the NPE explosion. We propose to represent the nonspherical secondary radiation that is produced by our model as an equivalent CLVD, thereby interpreting the Stevens et al. [10] result in terms of physical properties of the source medium that lead to asymmetry such as prestress, fracture anisotropy, and the depth dependence of confining stress, an effect we have not yet explored using our model.

Our focus on the effects of fracture damage on seismic coupling has motivated a program of field experiments in a Barre Granite quarry run by Weston Geophysical and New England Research termed the Vermont/New England Damage Experiment, or "NEDE". Of particular interest was the observed dependence of both the induced damage and the S wave radiation on the burn-rate (loading rate) of the explosive. Also interesting is the possibility that the lithostatic gradient promotes preferential fracture toward the free surface resulting in the creation of a compensated linear vector dipole "CLVD" contribution to the source, and a possible anisotropy in the dynamic damage caused by a known alignment of the initial factures (rift) in the Barre Granite [11], which is also a potential source of S radiation.

The ultimate goal of our research program is to develop and verify a physical model for the generation of fracture damage at the source that can calculate the generation of secondary high frequency P and S waves for a variety of rock types and tectonic environments, and to assess their effect on current P/S discriminants.

3. METHODS, ASSUMPTIONS, AND PROCEDURES

We use the micromechanics developed by Ashby and Sammis [8] and expanded by Deshphane and Evans [12] which considers an isotropic elastic solid containing an array of penny shaped cracks all of radius a and all aligned at an angle Ψ to the largest remote compressive stress σ_1 (Fig.1). Sliding on the array of penny-shaped cracks in Fig. 1 produces a wedging force F_w that drives tensile wing cracks to open in the direction of the smallest principal stress σ_3 and propagate parallel to the largest principal stress σ_1. Growth of wing cracks is enhanced by σ_1, retarded by σ_3, and enhanced by a global interaction that produces a mean tensile stress $\sigma_3^{(i)}$. The positive feedback provided by this tensile interaction stress leads to a run-away growth of the

wing cracks and ultimate macroscopic failure. The size and density of the initial flaws are characterized by an initial damage defined as

$$D_o = \frac{4}{3}\pi N_V (a\alpha)^3 \tag{1}$$

where N_V is the crack density (cracks per unit volume) and αa is the projection of the crack radius a in a vertical plane.

Wing cracks nucleate when the largest principal stress reaches a critical value given by:

$$\sigma_{1c} = \frac{\left[\left(1+\mu^2\right)^{1/2} + \mu\right]}{\left[\left(1+\mu^2\right)^{1/2} - \mu\right]}\sigma_3 - \frac{\sqrt{3}}{\left[\left(1+\mu^2\right)^{1/2} - \mu\right]}\frac{K_{Ic}}{\sqrt{\pi a}} \tag{2}$$

Crack growth is controlled by sliding on the cracks, which is controlled by the coefficient of friction μ. We ignore the difference between static and dynamic friction. We also assume that $\psi = 45^o$ and, hence, α=0.7. As the length of the wing cracks l grows, damage increases as

$$D = \tfrac{4}{3}\pi N_V (l + a\alpha)^3 \tag{3}$$

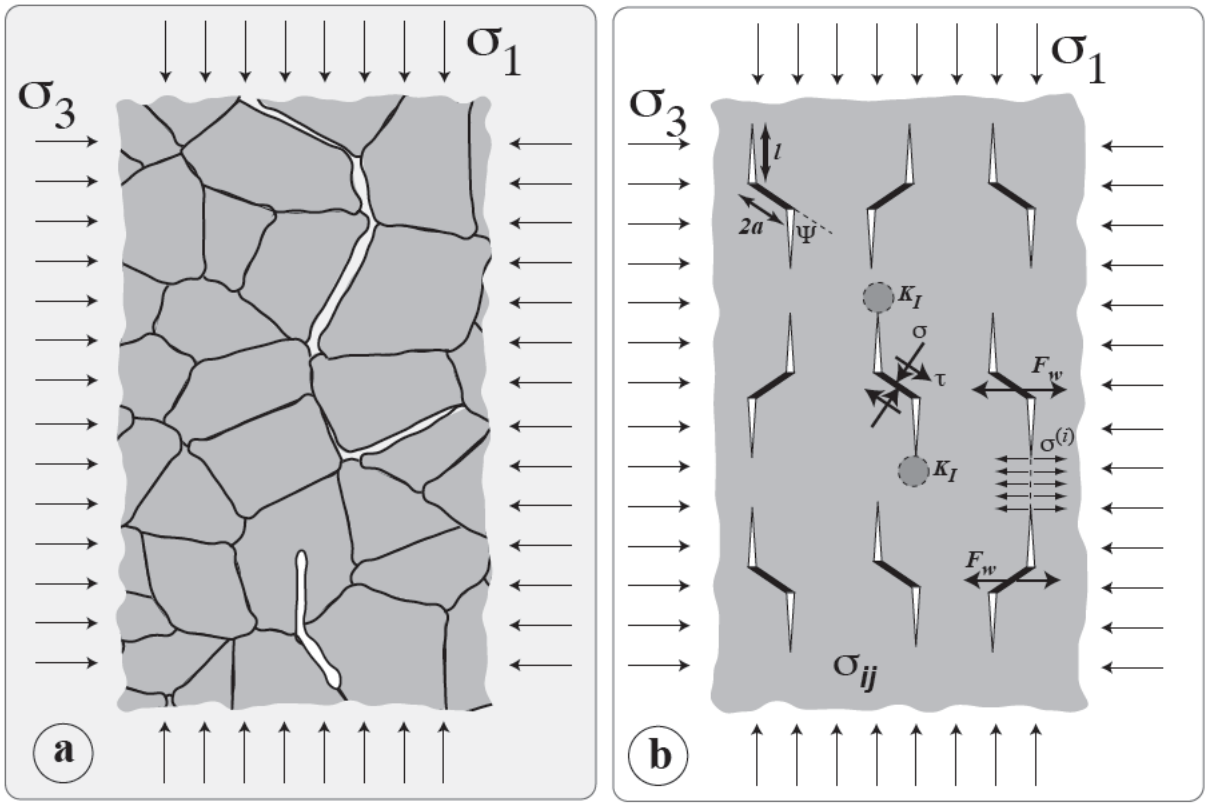

Figure 1: Geometry in the Micromechanical Damage Mechanics Model

Ashby and Sammis [8] show that, under these assumptions, the stress intensity factor at the tips of the growing wing cracks is

$$\frac{K_I}{\sqrt{\pi a}} = (\sigma_3 A_3 - \sigma_1 A_1)(c_1 + c_2) + \sigma_3 c_3 \tag{4}$$

where

$$A_1 = \mu\sqrt{\frac{b}{3}}\left[\left(1+\mu^2\right)^{1/2} - \mu\right] \qquad A_3 = A_1 \frac{\left[\left(1+\mu^2\right)^{1/2} + \mu\right]}{\left[\left(1+\mu^2\right)^{1/2} - \mu\right]} \tag{5}$$

and

$$c_1 = \frac{1}{p^2 a^{3/2}\left[\left(D/D_o\right)^{1/3} - 1 + b/a\right]^{3/2}}$$

$$c_2 = \frac{2}{p^2 a^{3/2}}\left[\left(D/D_o\right)^{1/3} - 1\right]^{1/2}\left(\frac{D_o^{2/3}}{1 - D^{2/3}}\right)$$

$$c_3 = \frac{2}{p}\sqrt{a}\left[\left(D/D_o\right)^{1/3} - 1\right]^{1/2} \qquad (6)$$

The original Ashby and Sammis formulation [8] is quasistatic. It assumes that wing cracks nucleate as soon as equation (2) is satisfied and that the their length is always given by the value of l that makes K_I in equation (4) equal to the critical stress intensity factor K_{Ic} (which is a constant for a given material). While this assumption is adequate for triaxial experiments at relatively low loading rates (which were fit by Ashby and Sammis [8]), it is a poor assumption at the high loading rates that typically occur in the non-linear source region of an explosion (or near an earthquake rupture front, or during an meteorite impact).

When Johnson and Sammis [7] used this damage mechanics to model the NPE experiment, we had to use an iterative approach in which we 1) solved the elastic problem, 2) calculated the equilibrium fracture damage from the stress, 3) adjusted the elastic constants for the damage, and then 4) returned to step 1. This iteration loop was repeated until the damage, stress, and elastic moduli became self-consistent.

However, at high loading rates, the nucleation and growth of cracks can't keep pace with the rapidly increasing stress field and true rate effects become important. Deshpade and Evans [12] introduced a simple *ad hoc* crack growth law into the Ashby/Sammis [8] damage mechanics to introduce such rate effects into their simulation of impacts on ceramic armor plating.

3.1 Extending Micromechanical Damage Mechanics to High Loading Rates

Working with Professor Ares Rosakis (chair of the engineering division at Caltech and an expert in high-speed crack growth), we have replaced Deshpande and Evans [12] *ad hoc* crack growth law with one based on the following theoretical and experimental considerations.

For a stationary finite crack under transient loading conditions the dynamic stress intensity factor, K_I^d evolves with time following the application of loads. Figure 2 shows the evolution of K_I^d scaled by its static limit. The abscissa, $c_R t/b$, denotes the time from the beginning of loading to the instant at which fracture initiation occurs scaled by the Rayleigh wave speed c_R and the crack half-length b.

As illustrated in Fig. 2, K_I^d rises sharply with time, overshoots the equivalent static value K_{st} by a considerable amount, and then oscillates around the static value with decreasing amplitude. This oscillation is due to the Rayleigh waves traveling back and forth along the surface of the crack with decreasing intensity.

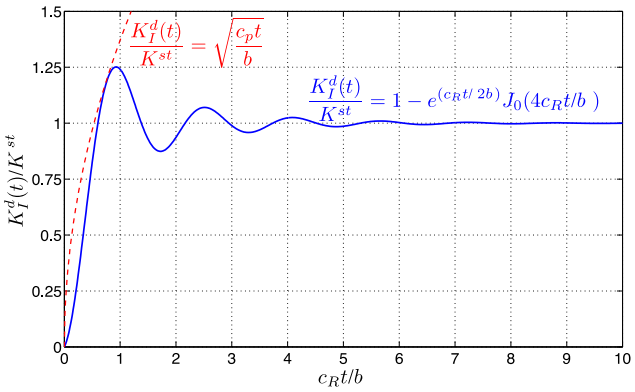

Figure 2: Temporal Evolution of the Dynamic Stress Intensity Factor

As a material parameter, K_{IC} can only be obtained through experimental measurements and is found to vary with loading rate. Figure 3a shows the critical value of the stress intensity factor K_I (scaled by its steady-state value) for crack nucleation as a function of loading rate. Loading rate is given by the scaled value of the time derivative of the dynamic stress intensity factor. Figure 3b shows the critical value of scaled K_I for crack propagation as a function of propagation velocity v.

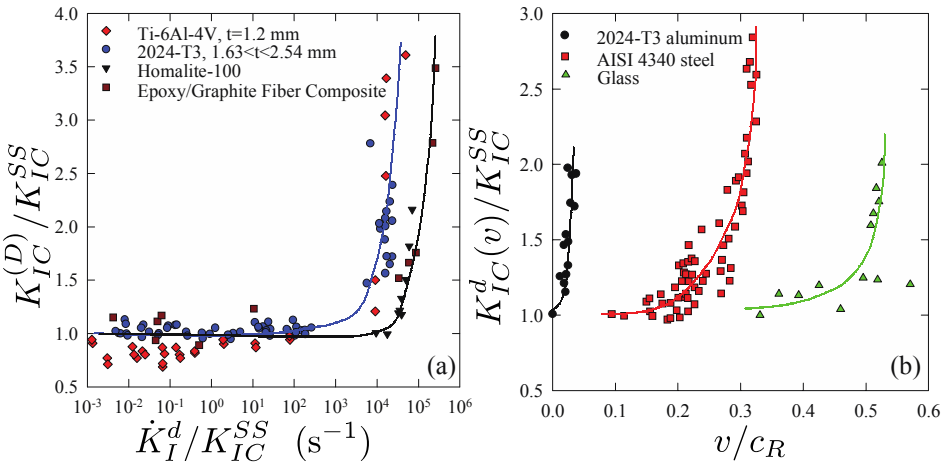

Figure 3: Normalized Dynamic Stress Intensity Factors for Several Materials

An expression that represents the dynamic behavior in Figs. 3a,b and Freund`s [13] result on the dynamic stress intensity factor of a growing crack have been incorporated into a user developed material subroutine (VUMAT) in ABAQUS to replace the ad-hoc growth law currently used by Deshpande and Evans [12].

3.2 Experimental Validation of Dynamic Damage Mechanics

Figure 4 shows the failure strength σ_p as a function of loading strain rate $d\varepsilon/dt$ in Dionysus-Pentelicon marble (from the Parthenon). The data are unpublished results of uniaxial and Hopkinson split bar experiments that are presented in our recent paper [14].

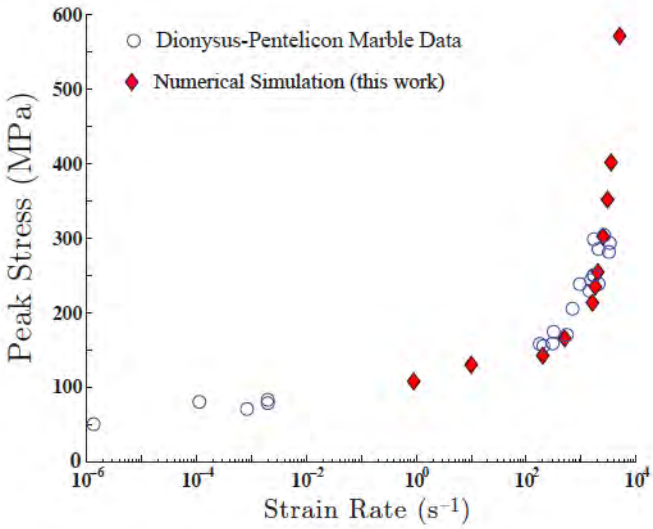

Figure 4: Comparison Between Experimental Measurements and Model Predictions

This result shows the power of our micromechanical model. Only two model parameters are required (the inital crack density *Do* and flaw size *a*), which were determined from the quasistatic uniaxial data at low strain rates near 10^{-6} s^{-1}. The diamonds are the model predictions at high loading rates, which clearly capture the sudden increase in strength at very high loading rates (as are typical in the non-linear source region of underground nuclear explosions).

4. RESULTS AND DISCUSSION

Figure 5 shows 2D simulations of an explosion using our new dynamic damage mechanics. A pressure pulse is applied to the surface of a 1 m diameter cavity in a rock with initial damage *Do* = 0.1. The insets show the time history of this pressure pulse. First note that the patterns show both circumferential and radial fracturing close into the explosion and a few radial fractures that extend to greater distances. Comparison with fracture maps from underground nuclear explosions in Fig. 6 and a simulated laboratory explosion in Fig. 7 show that we are, for the first time, correctly modeling the damage morphology. We simulate explosions in the lab by impacting plates with hypervelocity projectiles traveling faster than the speed of sound in the plate.

Note that Fig. 5 also shows the effect of the rise time and the duration. The amplitude of the stress determines the extent of the circumferential cracking while the duration determines the extent of the radial fractures. Figure 8 shows the displacement field generated by faster loading on the left and slower loading on the right. Note that the slow loading produces more radial fracturing and stronger S waves. This is in agreement with field observations in the NEDE quarry experiment which found that slow burning explosive produced stronger S waves. Based on the model, the physical interpretation is that the S waves are produced by asymmetry in the radial fractures.

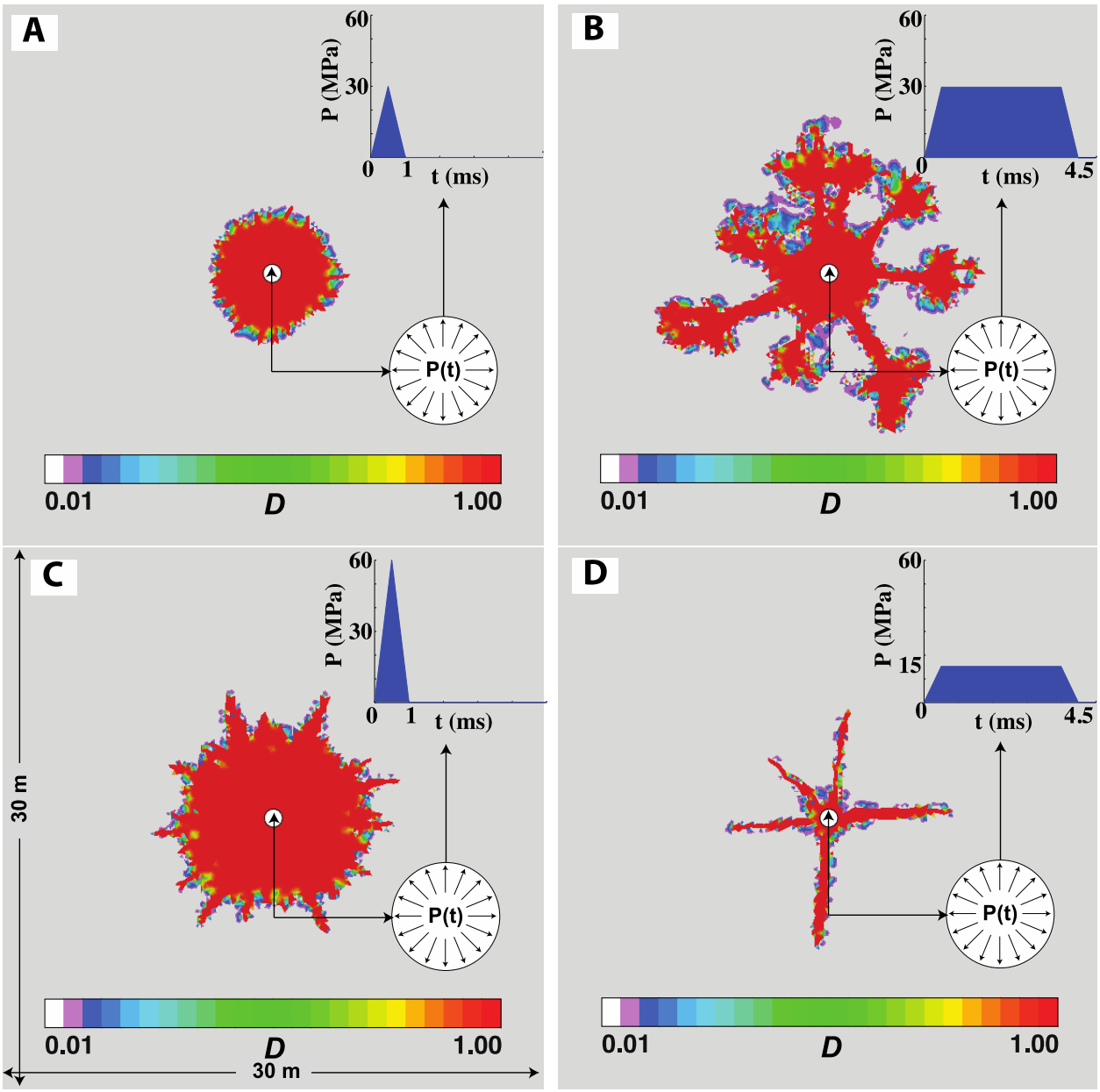

Figure 5: Dynamic Damage Created by Different Loading Regimes

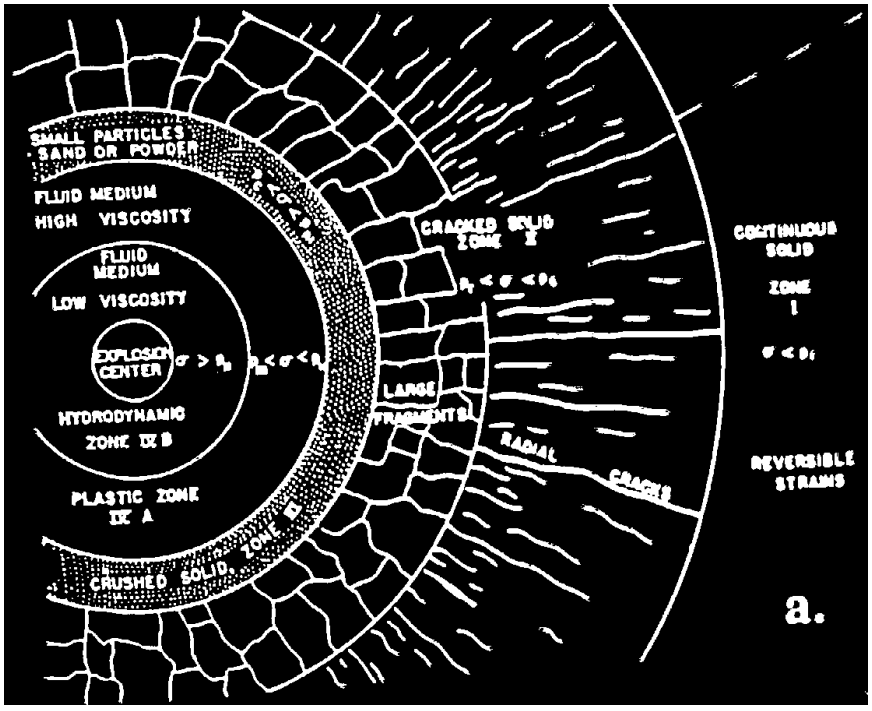

Figure 6: Damage Mapped in the Source of a Nuclear Explosion

Figure 7: Damage in a Glass Plate Produced by a Hypervelocity Impact

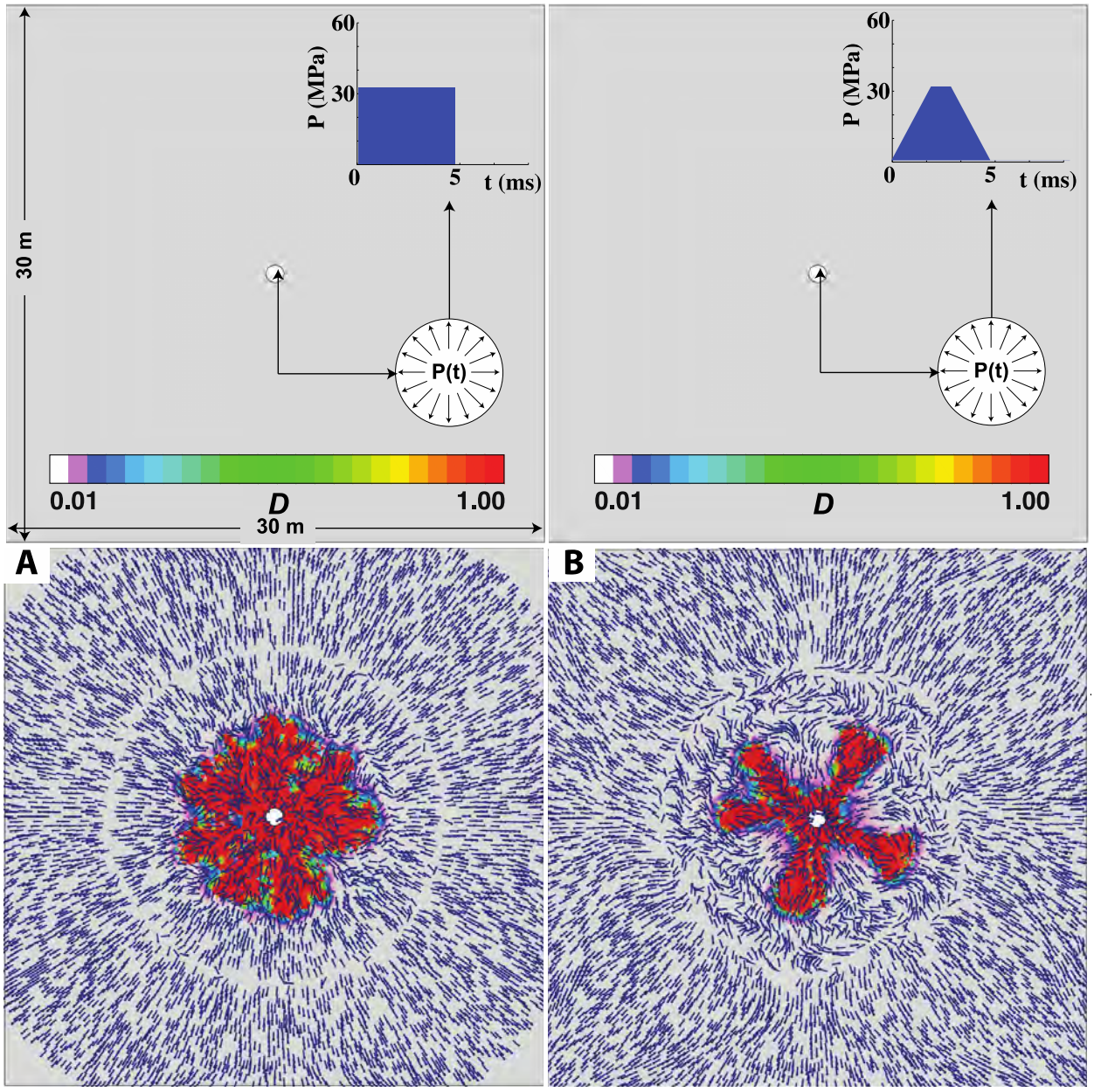

Figure 8: Displacement Fields Generated by Fast Loading (Left) and Slow Loading (Right)

The Ashby/Sammis damage mechanics upon which all this work is based is sometimes criticized because it assumes that all the active flaws have the same size and orientation. In Bhat et al. [15] we focused on Westerly Granite (one of the most studied rocks) and explored the effects of allowing a range of flaw sizes and orientations consistent with petrologic studies. We found that relaxing the assumption of a single flaw size and orientation had little or no effect on the predicted failure surface. The reason is that variations in size and orientation are compensated by an increase in the density of flaws that are required to fit the uniaxial strength. We also

discovered that curvature observed in the triaxial failure surface is caused by plastic flow of the weaker minerals in the granite, and thus can be ignored at the extremely high dynamic stresses in the source region of an explosion.

5. CONCLUSIONS

Loading-rate plays an important role in the spatial extent and pattern of fracture damage, and, consequently, in the generation of secondary P and S waves in the non-linear source region of underground explosions. It is therefore important that effects of loading rate on the nucleation and growth of fracture damage be included in simulations of underground explosions. The micromechanical model developed here does this in a physical way that incorporates information on the source rock such as the size and density and anisotropy of the initial fractures and information about the source environment such as lithostatic pressure and water (or ice) in the initial cracks.

While we have built our new dynamic damage mechanics into the ABAQUS dynamic finite element code, it should be emphasized that the ultimate goal of our work is *not* to produce a new numerical code to simulate underground nuclear explosions. Rather, the goal has been to validate the dynamic damage mechanics by comparison with lab experiments and identify first-order consequences for seismic coupling. Our ultimate goal is to develop a damage mechanics that captures the physics of S wave generation and that can be incorporated in current (and more sophisticated) numerical simulators. We have collaborated with the relevant private contractors and national labs in the past to incorporate the quasistatic Ashby/Sammis damage mechanics and plan to continue these collaborations.

REFERENCES

[1] Bouchon, M., "The Complete Synthesis of Seismic Crustal Phases at Regional Distances," *J. Geophys. Res*., **87**, 1982, pp. 1735-1741.

[2] Knopoff, L., Schwab, F., and Kausel, E., "Intepretation of *Lg," Geophys. J. R. Astron. Soc.,* **33**, 1973, pp. 983-993.

[3] Walter, W. R., Mayeda, K. M., and Patton, H. J., "Phase and Spectral Ratio Discrimination Between NTS Earthquakes and Explosions; Part I, Empirical Observations," *Bull. Seism. Soc. Am.*, **85**, 1995, pp. 1050-1067.

[4] Press, F. and Archambeau C., "Release of Tectonic Strain by Underground Nuclear Explosions," *J. Geophys. Res.,* **67**, 1962, pp. 337-343.

[5] Töksoz, M. N., Harkrider, D. J., and Ben-Menahem, A., "Determination of Source Parameters by Amplitude Equalization of Seismic Surface Waves, 2. Release of Tectonic Strain by Underground Explosions and Mechanisms of Earthquakes," *J. Geophys. Res*., **70**, 1965, pp. 907-922.

[6] Archambeau, C. and Sammis, C. G., "Seismic Radiation from Explosions in Prestressed Media and the Measurement of Tectonic Stress in the Earth," *Rev. Geophys. Space Phys.,* **8**, 1970, pp. 473-499.

[7] Johnson, L. R. and Sammis, C. G., "Effects of Rock Damage on Seismic Waves Generated by Explosions," *Pure Appl. Geophys.*, **158**, 2001, pp. 1869-1908.

[8] Ashby, M. F. and Sammis, G. G., "The Damage Mechanics of Brittle Solids in Compression," *Pure Appl. Geophys*., **133**, 1990, pp. 489-521.

[9] Xie, J. and Patton, H. J., "Regional Phase Excitation and Propagation in the Lop Nor Region of Central Asia and Implications for P/Lg Discriminates," *J. Geophys. Res*., **104**, 1999, pp. 941-954.

[10] Stevens, J. L., Baker, C. E., Xu, H., Bennett, T. J., Rimer, N., and Day, S. M., "The Physical Basis of Lg Generation by Explosion Sources," *Proceedings of the 25th Seismic Research Review*, 2003, p. 456.

[11] Engelder, T., Sbar, M. L., and Kranz, R., "A Mechanism for Strain Relaxation of Barre Granite: Opening of Microfractures," *Pure Appl. Geophys.*, **115**, 1977, pp. 28-40.

[12] Deshpande, V. S. and Evans, A. G., "Inelastic Deformation and Energy Dissipation in Ceramics: A Mechanism-Based Constitutive Model," *J. Mech. Phys. Solids*, **56**, 2008, pp. 3077–3100.

[13] Freund, L. B., "Crack Propagation in an Elastic Solid Subjected to General Loading-III: Stress Wave Loading," *J. Mech. Phys. Solids*, **21**, 1973, pp. 47–61.

[14] Bhat, H. S., Rosakis, A. J. and Sammis, C. G., "A Micromechanics Based Constitutive Model For Brittle Failure at High Strain Rates," *J. Appl. Mech. Rice Special Volume*, 2012, in press.

[15] Bhat, H. S., Sammis, C. G. and Rosakis, A. J., (2011), "The Micromechanics of Westerley Granite at Large Compressive Loads," *Pure and Appl. Geophys*, **168**, 2011, pp. 2181-2198.

DISTRIBUTION LIST

DTIC/OCP
8725 John J. Kingman Rd, Suite 0944
Ft Belvoir, VA 22060-6218 1 cy

AFRL/RVIL
Kirtland AFB, NM 87117-5776 2 cys

Official Record Copy
AFRL/RVBYE/Robert Raistrick 1 cy